Journal Name

ARTICLE TYPE

Cite this: DOI: 10.1039/xxxxxxxxxx

Stress Fluctuations in Transient Active Networks†

Daniel Goldstein,*[a] Sriram Ramaswamy,[b‡] and Bulbul Chakraborty[a]

Received Date
Accepted Date

DOI: 10.1039/xxxxxxxxxx

www.rsc.org/journalname

Supplemental Information

0.0.0.1 Connectivity After a period of 2-4 spring lifetimes we find that the distribution of network connectivity, $P(z)$, settles to a time-independent form, which can be represented by a power law with an exponent of -1 and an exponential cut off that depends on s_{max}. A set of steady state connectivity distributions can be seen in Fig. 1 for s_{max} (denoted by color) ranging from $s_{max} = 10 \ldots 50$ and $\alpha = 0.05 \ldots 10$. As seen in the figure, the cutoff in $P(z)$ is controlled primarily by s_{max} with a much weaker dependence on the activity, α.

0.0.0.2 Stress distribution in steady state We find that the probability of finding a spring of age t_b at a length ℓ in the steady state $P(l,t_b)$, near the peak, can be fit by a Gaussian of the form:

$$P(\ell,t_b) = \frac{1}{\sqrt{2\pi b t_b^{3/2}}} \exp\left(-\frac{(at_b+1-\ell)^2}{2(b_1 t_b + b_2 t_c^2)}\right) \quad (1)$$

The equilibrium length of an active spring that has been growing for a time t_b is $s = \alpha t_b + 1$, which implies that the stress that has built up in the spring is: $\sigma(t_b,\ell) = k(\alpha t_b + 1 - \ell)\ell$. Using this equation we can perform a simple change of variables to obtain a conditional distribution for the trace of the stress tensor, Π.

$$P(\Pi,t_b) = \frac{\exp\left(-\frac{\left(\sqrt{k}(2at_b - \alpha t_b + 2) + \sqrt{\alpha^2 k t_b^2 - 4\Pi}\right)^2}{8k(b_1 t_b + b_2 t_b^2)}\right) + \exp\left(-\frac{\left(\sqrt{k}(-2at_b + \alpha t_b - 2) + \sqrt{\alpha^2 k t_b^2 - 4\Pi}\right)^2}{8k(b_1 t_b + b_2 t_b^2)}\right)}{\sqrt{2\pi}\sqrt{k(b_1 t_b + b_2 t_b^2)}\sqrt{|k t_b^2 \alpha^2 - 4\Pi|}} \quad (2)$$

This stress distribution is doubly peaked. There is a sharp peak at $\Pi = k t_b^2 \alpha^2/4$ the maximum value the stress can have for a spring of a given age. The mean of this stress distribution is at $k\alpha t_b(at_b - 1) - k(b_1 t_b + b_2 t_b^2)$. Notably there is a large population under a lot of stress and the mean of this distribution increases with time. Negative stress here denotes that a spring is over extending and exerting a contractile force while positive stress denotes the spring is applying an extensile force. Some examples of these conditional distributions are presented in Fig. 3. By convolving this distribution with the survival probability, $P_s(t)$, of the springs in the system we can obtain the stress distribution in steady state.

$$P(\Pi) = \int dt_b P_s(t_b) P(\Pi,t_b)\ , \quad (3)$$

The survival probability $P_s(t_b)$ and the failure probability $P_f(t_b)$ are related to each other and to the *lifetime* distribution, $P_l(t)$, which is what we prescribe to define the model. We deduce $P_s(t)$ from the prescribed Gaussian form of $P_l(t)$, as outlined below. The probability that a spring will survive to an age $t_b + \delta t_b$ is equal to the probability that it has survived until age t_b and then does not fail in a time interval δt_b.

$$P_s(t_b + \delta t_b) = P_s(t_b)(1 - \delta t_b P_f(t_b)) \quad (4)$$

$$\frac{1}{\delta t}(P_s(t_b + \delta t_b) - P_s(t_b)) = P_s(t_b) P_f(t_b) \quad (5)$$

$$\frac{\mathrm{d}P_s(t_b)}{\mathrm{d}t_b} = -P_s(t_b) P_f(t_b) \quad (6)$$

By assigning a lifetime to each bundle, we are prescribing the probability that a spring has failed exactly at time t_b, i.e., the probability that a spring has survived until age t_b then fails. This distribution, $P_l(t_b) = P_s(t_b) P_f(t_b)$, we have prescribed to be a Gaussian:

$$P_l(t_b) = \frac{e^{\frac{-(t_b-\tau)^2}{(2(\alpha s_0+\tau)/4)^2)}}}{\sqrt{2\pi((\alpha s_0+\tau)/4)^2}} \ . \tag{7}$$

Using this form leads to a survival probability of

$$P_s(t_b) = \frac{1-\mathrm{erf}(2^{3/2}\frac{t_b-\tau}{\tau})}{2\tau} \tag{8}$$

The stress distribution in steady state, which is independent of time, is obtained from Eq. 3 by using $P_s(t_b)$ obtained from the above equation, and the numerically evaluated distribution of lengths in steady state, $P(l,t_b)$, shown in Fig. 3 of the main text. Additionally, by convolving the conditional stress distribution with the lifetime distribution, we can define an effective yield stress distribution. This is not a true yield stress as putting more stress on a spring will not cause it to break, it is simply the stress springs are under at the moment of their death dictated by the lifetime assigned at birth. Fig. 2 in the main text compares the measured stress distribution with the forms predicted by the above analysis. In the next section, we present our solution to the stochastic differential equation representing the effective medium.

0.0.0.3 SDE Solution We provide details of the calculation of the stochastic differential equation that we have used to model $P(l,t_b)$. To get a sense of how a system behaves we first consider the floppy limit of the spring, $k \to 0$

$$\frac{\mathrm{d}\ell}{\mathrm{d}t_b} = -\ell\eta \tag{9}$$

we can solve this equation though a change of variables $\ell = e^y$ now $\frac{\mathrm{d}\ell}{\mathrm{d}t_b} = \frac{\mathrm{d}y}{\mathrm{d}t_b}\ell$ and $\frac{\mathrm{d}y}{\mathrm{d}t_b} = -\eta$. Now if we want to find $\langle\ell\rangle = \langle e^y\rangle$ we can use a cumulant expansion to write down $log(\langle\ell\rangle) = log\langle e^y\rangle = -a_\eta t_b + Dt_b$. Thus $\langle\ell\rangle = e^{(-a_\eta+D)t_b}$, there is a relaxation timescale coming from the mean of the noise distribution as well as the variance. It is important to note here that this calculation was done using the notion of a Stratonovich[31] integral so the notion of the chain rule remains the same in the presence of multiplicative noise.

For a more complicated system of the form

$$\frac{\mathrm{d}\ell}{\mathrm{d}t_b} = f(t_b)\ell + g(t_b) - \ell\eta(t_b) \ , \tag{10}$$

one can make the transformation $\ell = z(t_b)\exp\left(\int_0^{t_b} f(s)ds + y(t_b)\right)$. We can then write

$$\frac{\mathrm{d}\ell(t_b)}{\mathrm{d}t_b} = \frac{\mathrm{d}z(t_b)}{\mathrm{d}t_b}\exp\left(\int_0^{t_b} f(s)ds + y(t_b)\right) + \ell(t_b)\left[f(t_b) + \frac{\mathrm{d}y(t_b)}{\mathrm{d}t_b}\right] \tag{11}$$

$$\ell\frac{\mathrm{d}y(t_b)}{\mathrm{d}t_b} + \frac{\mathrm{d}z(t_b)}{\mathrm{d}t_b}\exp\left(\int_0^{t_b} f(s)ds + y(t_b)\right) = g(t_b) - \ell\eta(t_b) \tag{12}$$

Thus by making the identification

$$\frac{\mathrm{d}z(t_b)}{\mathrm{d}t_b}\exp\left(\int_0^{t_b} f(s)ds + y(t_b)\right) = g(t_b) \tag{13}$$

$$z(t_b) = \int_0^{t_b} g(s)\exp\left(-\int_0^{s} f(s')ds' - y(s)\right)ds \tag{14}$$

We can then arrive at

$$\frac{\mathrm{d}y(t_b)}{\mathrm{d}t_b} = -\eta(t_b) \tag{15}$$

$$\ell(t_b) = \left[\ell(0) + \int_0^{t_b} g(s)\exp\left(-\int_0^{s} f(s')ds' - \int_0^{s}\eta(s')ds'\right)ds\right]\exp\left(\int_0^{t_b} f(s)ds - \int_0^{t_b}\eta(s)ds\right) \tag{16}$$

$$\ell(t_b) = \left[s_0 + \int_0^{t_b} 2\mu k(\alpha s + s_0)\exp\left(2\mu k t_b + \int_0^{s}\eta(s')ds'\right)ds\right]\exp\left(2\mu k s - \int_0^{t_b}\eta(s)ds\right) \tag{17}$$

0.0.0.4 Noise Parameters To complete the definition of our effective medium, we need to compute the parameters ω_η and ω_c, which define the mean and variance of the noise. We obtain the variation of these parameters with activity by fitting to results of simulations of the active spring model. The easiest way to obtain the values of ω_c and ω_η is to use the long time limits of the mean and variance of ℓ. Fitting the mean gives us a value for ω_{eff} and fitting the variance gives a value for ω_c. It is then simple to solve for ω_η. This process was carried out for values of α ranging from $\alpha = .01$ to $\alpha = 10$ and $s_{max} = 50$. For smaller values of s_{max}, it was difficult to obtain adequate statistics since very few springs reached the long-time limit. For each parameter value 20 different realizations were simulated and the values of ω_η and ω_c were averaged. A plot of these parameters for different values of α can be seen in Fig. 4.

A set of distributions of ℓ obtained from this effective medium theory can be seen in Fig. 5.

0.0.0.5 Elastoplastic Modeling The stress fluctuations observed in our model are reminiscent of those observed in shear-driven amorphous solids, which undergo plastic failure. A model that has been used to analyze plasticity in amorphous solids is a kineto-elastoplastic model. This model can be viewed as a "stress automaton" in which the solid is divided into mesoscopic elements each characterized by a yield stress picked from a distribution. Under externally imposed driving at a constant rate, the stress in each element, σ_i, builds up elastically until it reaches its yield stress. Beyond this the stress decays to zero with a characteristic time τ[29,30]. The stresses in the other units are then altered by an amount $\delta\sigma_j = G_{ij}\sigma_i$ according to a prescribed Green's function G_{ij}. The distribution of yield stresses and the Green's function parametrize the model.

We performed calculations using a stress automaton under periodic boundary conditions using the elastic Green's function, and the yield stress distribution obtained from our numerical simulations of the active spring model (Fig. 2 c in the main text). This specific yield stress distribution provides the connection between the strong nonaffine effects in the transient, active spring network, and the stress reorganization (diffusion) characteristic of the kineto-elastoplastic models, which envision each mesoscopic unit as deforming affinely all the way up to the yield stress. Results were obtained for $\dot{\gamma}\langle\tau\rangle = 1$ and $1/2$. Comparing the results for $P(\sigma)$, shown in Fig. 6, to $P(\Pi)$ shown in the main text, demonstrates that the basic mechanism of failure and redistribution of stress in an elastic medium captures the qualitative behavior observed in the active spring model including the cusp at small stress.

Notes and references

1 A Onuki, J. Phys.: Condens. Matt., 1997, **9**, 6119.
2 R M L Evans, R A Simha, A Baule & P D Olmsted, Phys. Rev. E, 2010, **81**, 051109.
3 A Dhar, Adv Phys, 2008, **57**, 457-537.
4 H.A. Barnes, J Non-Newtonian Fluid Mech., 1999, **81**, 133-178.
5 K.H. Nagamanasa, S. Gokhale, A.K. Sood, R. Ganapathy, Phys. Rev. E, 2014, **89**, 062308.
6 E Brown & H M Jaeger, Rep. Prog. Phys., 2014, **77**, 046602.
7 P.D. Olmsted, Rheol Acta, 2008, **47**, 283-300.
8 S M Fielding, Rep. Prog. Phys., 2014, **77**, 102601.
9 F. Tanaka and S. F. Edwards, Macromolecules, 1992, **25**, 1516.
10 S Ramaswamy Annu. Rev. Condens. Matter Phys., 2010 **1** 301.
11 G I Menon, in Rheology of Complex Fluids, eds J Murali Krishnan *et al.*, Springer, New York (2010).
12 É Fodor & M C Marchetti, *The statistical physics of active matter: from self-catalytic colloids to living cells* (Lecture notes for the international summer school "Fundamental Problems in Statistical Physics", Bruneck, 2017); Physica A, 2018, **504**, 106.
13 F. C. MacKintosh, C. F. Schmidt, Current Opinion in Cell Biology, 2010, **22**, 29.
14 K.-T. Wu, J. B. Hishamunda, D. T. N. Chen, S. J. DeCamp, Y.-W. Chang, A. Fernández-Nieves, S. Fraden and Z. Dogic, Science, 2017, **355**, eaal1979.
15 M. C. Marchetti, J. F. Joanny, S. Ramaswamy, T. B. Liverpool, J. Prost, M. Rao and R. A. Simha, Reviews of Modern Physics, 2013, **85**, 1143–1189.
16 David Saintillan & Michael J.Shelley, Comptes Rendus Physique, 2013, **14**, 497.
17 J. Prost, F. Jülicher & J-F. Joanny, Nature Physics, 2015, **11**, 111.
18 F. Jülicher, S. W. Grill and G. Salbreux Reports on Progress in Physics, 2018, **81**, 076601.
19 S. Banerjee and M. C. Marchetti, Soft Matter, 2011, **7**, 463–473.
20 D. S. Banerjee, A. Munjal, T. Lecuit and M. Rao, Nat Commun, 2017, **8**, 1121.
21 D. Saintillan, Annu. Rev. Fluid. Mech., 2018, **50**, 563–592.
22 T. Sanchez, D. T. N. Chen, S. J. DeCamp, M. Heymann and Z. Dogic, Nature, 2012, **491**, 431–434.
23 G. Henkin, S. J. DeCamp, D. T. N. Chen, T. Sanchez and Z. Dogic, Philosophical Transactions of the Royal Society A: Mathematical, Physical and Engineering Sciences, 2014, **372**, 20140142–20140142.
24 T. Sanchez, D. Welch, D. Nicastro and Z. Dogic, Science, 2011, **333**, 456–459.
25 F. Hilitski, Ph.D. thesis, Brandeis University, 2017.
26 T. Gao, R. Blackwell, M. A. Glaser, M. D. Betterton and M. J. Shelley, Physical Review E, 2015, **92**, year.
27 C. L. Kane and T. C. Lubensky, Nature Physics, 2013, **10**, 39–45.
28 A. W. Lees and S. F. Edwards, Journal of Physics C: Solid State Physics, 1972, **5**, 1921.
29 A. Nicolas, K. Martens, L. Bocquet and J.-L. Barrat, Soft Matter, 2014, **10**, 4648–4661.
30 G. Picard, A. Ajdari, F. Lequeux and L. Bocquet, Phys. Rev. E, 2005, **71**, 010501.
31 R. L. Stratonovich, SIAM Journal on Control, 1966, **4**, 362–371.

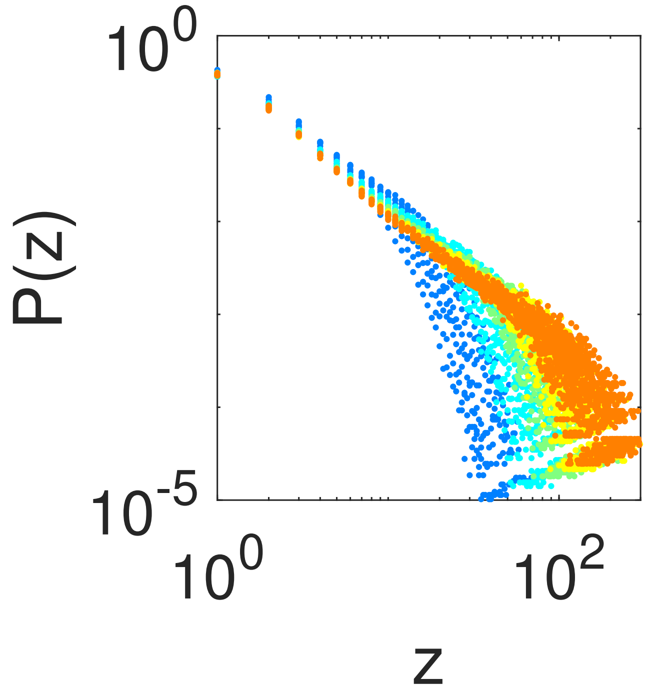

Fig. 1 P(z) for different values of α, and s_{max}. Colors correspond to different values of s_{max}: Blue - $s_{max} = 10$, Teal - $s_{max} = 20$, Yellow - $s_{max} = 30$, Orange - $s_{max} = 40$. The spread of points with a given color reflects the variation with activity for $\alpha = 0.05 \ldots 10$.

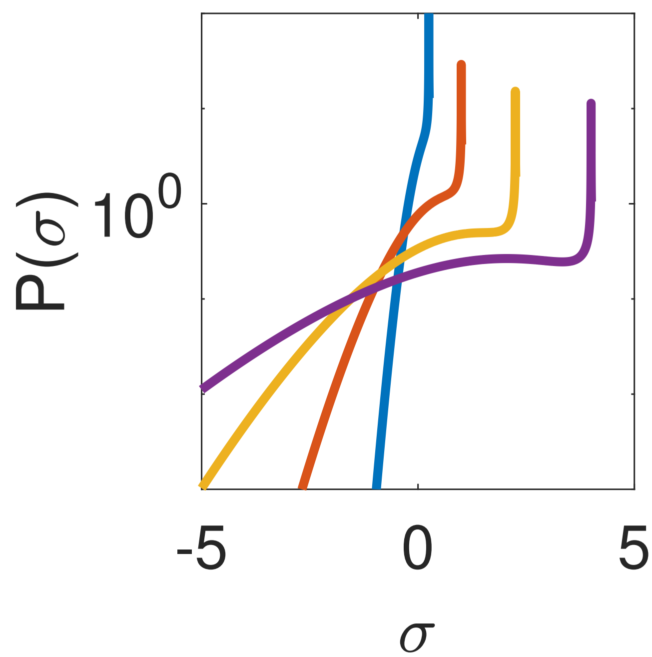

Fig. 3 $P(\Pi, t_b)$ for different values of t_b. Blue - $t_b = 1$, Red - $t_b = 2$, Yellow- $t_b = 3$, Purple- $t_b = 4$,

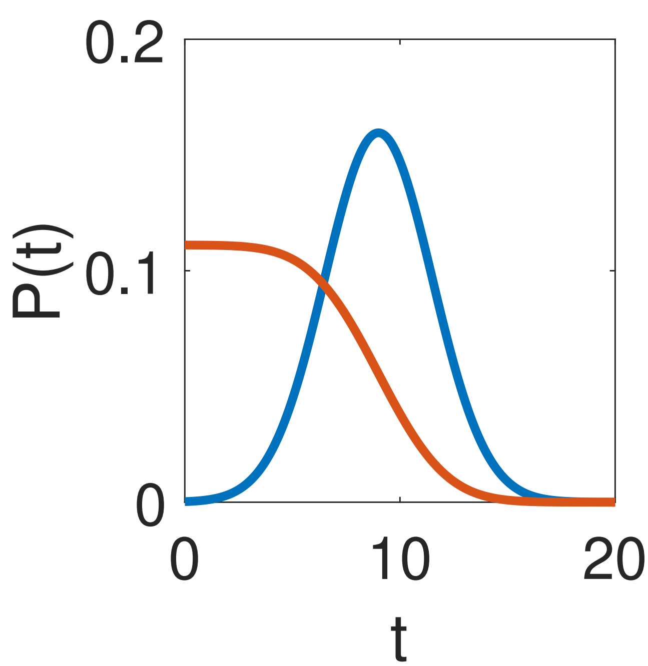

Fig. 2 Blue - Life time distribution, $P_l(t)$, of springs for $s_{max} = 10$, $\alpha = 1$, $\langle \tau \rangle = 9$. Red - The corresponding survival time distribution obtained from Eq. 8.

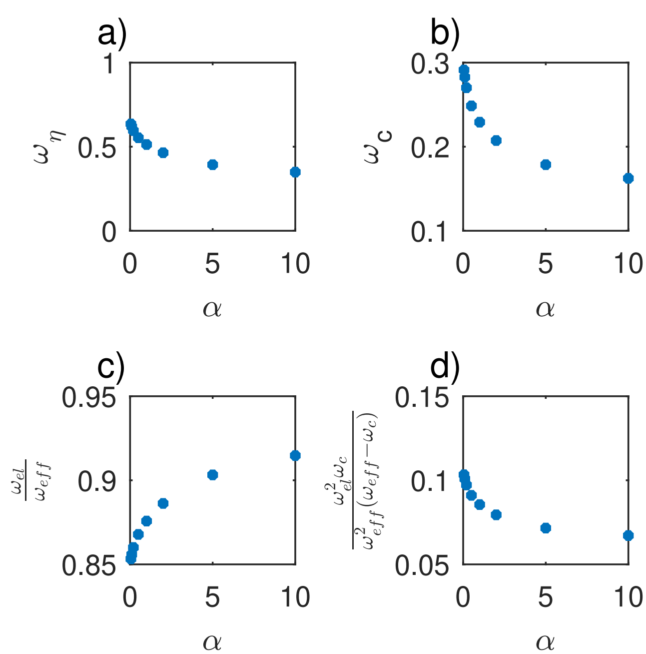

Fig. 4 Values of noise parameters as a function of α for $s_{max} = 50$.

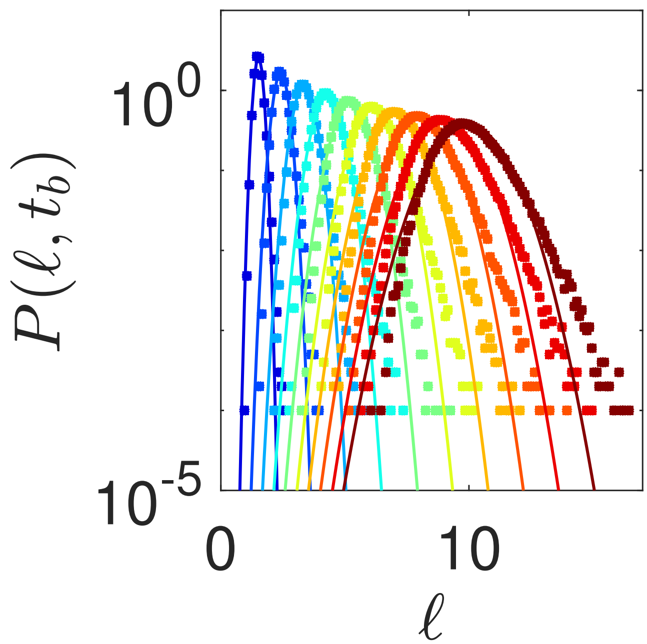

Fig. 5 A set of length distributions of the spring from the effective medium theory conditioned on how long they have existed. Plots are shown for $t_b = (1,2,3,4,5,6,7,8,9,10)$ for a system where $s_{max} = 10$. Gaussian fits of the regions near the peaks are shown as solid lines.

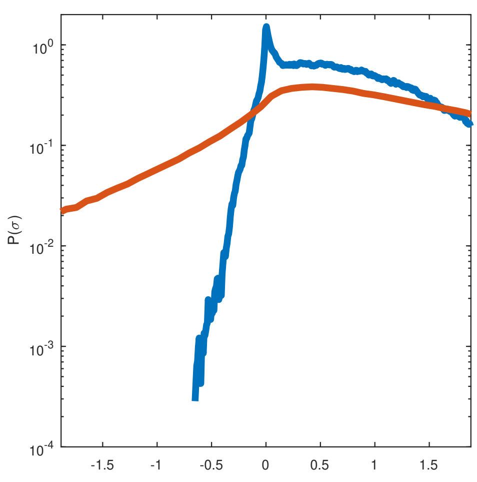

Fig. 6 Distribution of σ (blue line) obtained from simulations of the elasto-plastic miodel using the yield stress distribution computed from the active springs model with peak scaled to an arbitrary value (red line), which sets the stress scale for the automaton. These results were obtained for $\dot{\gamma}\langle\tau\rangle = 1$.